

# More on thermal holographic RG flows in a 3D gauged supergravity

Anastasia A. Golubtsova<sup>a,b1</sup>, Eric Gourgoulhon<sup>c,d2</sup> and Mikhail A. Podoinitsyn<sup>a3</sup>

<sup>a</sup> *Bogoliubov Laboratory of Theoretical Physics, JINR,  
Joliot-Curie str. 6, Dubna, 141980 Russia*

<sup>b</sup> *Steklov Mathematical Institute, Russian Academy of Sciences  
Gubkina str. 8, 119991 Moscow, Russia*

<sup>c</sup> *LUTH, UMR CNRS 8102, Observatoire de Paris, Université PSL, Université Paris Cité, 5 place  
Jules Janssen, 92190 Meudon, France*

<sup>d</sup> *Laboratoire de Mathématiques de Bretagne Atlantique, UMR CNRS 6205, Université de Bretagne  
Occidentale, 6 avenue Victor Le Gorgeu, 29200 Brest, France*

## Abstract

We continue our studies of holographic renormalization group (RG) flows for a 3d truncated supergravity model, the scalar potential of which can have either one or three extrema depending on the radius of the target manifold. We construct numerically and analytically thermal holographic RG flows, which are described by asymptotically AdS<sub>3</sub> black holes (non-rotating BTZ) characterized by the value of the scalar field on the horizon. We find two classes of RG flows with monotonic and non-monotonic behavior of the scalar field. The first one exists for both types of the potential, while the second one appears only for the potential with three extrema. For the slowly changing scalar field we find a special class of RG flows, which are described by the scalar field in the BTZ black hole geometry. For such flows we present an analytic solution for the scalar field from the horizon to the boundary. We discuss thermodynamical properties of the constructed holographic RG flows.

---

<sup>1</sup>golubtsova@theor.jinr.ru

<sup>2</sup>eric.gourgoulhon@obspm.fr

<sup>3</sup>mpod@theor.jinr.ru

<b>1</b>	<b>Introduction</b>	<b>3</b>
<b>2</b>	<b>Setup</b>	<b>4</b>
2.1	The holographic model . . . . .	4
2.2	The dynamical system in $\mathbf{R}^3$ . . . . .	7
2.3	The dynamical system in the cylinder . . . . .	7
<b>3</b>	<b>Asymptotically AdS (BTZ) black hole solutions</b>	<b>10</b>
3.1	Exact BTZ black holes . . . . .	10
3.2	Near-horizon asymptotically AdS black holes . . . . .	10
3.3	Thermodynamics of the near-horizon solutions . . . . .	12
<b>4</b>	<b>From the near-horizon region to the boundary</b>	<b>15</b>
4.1	Analytic solutions from the horizon to the boundary . . . . .	15
4.2	The behaviour of the scalar field near boundary . . . . .	18
<b>5</b>	<b>Discussion</b>	<b>19</b>
<b>A</b>	<b>Exact holographic RG flow</b>	<b>21</b>
<b>B</b>	<b>BTZ black hole in various coordinates</b>	<b>21</b>

# 1 Introduction

The holographic duality [1–3] is a tool that allows to describe various aspects of physical systems under strong coupling using gravity.

In the holographic prescription a RG flow [4] can be represented as a Poincaré invariant (domain wall) solution with AdS asymptotics and appropriate boundary conditions for the field content [5–13]. The extrema of the scalar potential, where the geometries are AdS spacetimes, associate with fixed points of the dual field theory, which are deformed either by a relevant operator or by non-zero VEV of the operator.

Thermal RG flows encodes an information on a physical system and may shed light on puzzling properties of exotic RG flows. Finite temperature generalization of holographic fixed points is represented by AdS black holes. Holographic RG flows were studied broadly for the phenomenological applications in [14–22]. Another direction of using thermal RG flows in holographic theories is to probe the interior of the black hole in the gravitational dual [23–25].

In this paper we continue studies of holographic RG flows at finite temperature in 3d gauged supergravity coupled to a single scalar field with a potential [26, 27], which were constructed in [28]. Despite a simple form of the model it includes interesting features that can be realized in more sophisticated supergravity constructions. The scalar potential can have either one or three extrema depending on the value of the parameter related with the radius of the scalar target manifold. An exact domain wall solution for this model, describing half-supersymmetric RG flow was found in [27]. In works [29, 30] string solutions for this model were constructed. In [31, 32] holographic RG flows at zero temperature for this model were studied reducing the equations motion to an autonomous dynamical system using the scalar variables [18]. In [32] for RG flows driven by the relevant operator as well as non-zero VEV with various boundary conditions (Dirichlet, Neumann, mixed) "pseudo"-superpotentials were found.

Note, that the reconstruction of the (super)gravity solutions from the analysis of fixed points of the dynamical systems was discussed in [17, 33, 34]. In particular, finding domain wall solutions with zero and finite temperatures for the truncated supergravity model were performed in [28, 31, 32].

Holographic RG flows, constructed in [28], are thermal generalization to those from [31, 32]. These flows involve some numerical input. The equations of motion are represented as an autonomous dynamical system which configuration space is a unit cylinder. In such configuration space near-horizon regions of the solutions are mapped on the line of the boundary of the cylinder. Numerical black hole solutions are constructed such that for the initial conditions we used the constraints for the coordinates and the value of the scalar field on the horizon. In [28] it was shown that a separatrix for the constructed asymptotically AdS black holes for the case of the potential with one extremum is the supersymmetric zero-temperature RG flow [27] between AdS and scaling fixed points, while for the case of the potential with three extrema the separatrix

is the non-supersymmetric zero-temperature RG flow between two AdS fixed points. Moreover, using the cylinder for the configuration space allows to construct analytic near-horizon solutions, which have AdS asymptotics. From the analysis of the scalar field dynamics it was established special class of the flows, for which one can assume an additional constraint yielding an analytic solution for the scalar field from the boundary to the horizon. An interesting point is that under this constraint the geometry does not have a deformation and is described by the BTZ metric, while the scalar field is given by the solution to the hypergeometric equation.

The outline of the paper is as follows. In Section 2 we review the holographic model, which scalar potential depends on the parameter  $a^2$ , and write down equations of motion using a black hole ansatz in the domain wall coordinates. Then we present the equations of motion in different configuration spaces. In Section 3 we construct a near-horizon asymptotically AdS<sub>3</sub> black hole from the dynamical system and discuss its thermodynamical properties. In Section 4 we find of a special class of RG flows with the condition that the scalar field slowly changes. Such solution can be represented analytically from the horizon to the boundary. We also explore the behaviour of the solution for the scalar field of the boundary and show that it is in agreement with known results. In Section 5 we give a discussion of the results and future directions.

Some of the computations in this article have been performed by means of the computer algebra system SageMath [35]; the relevant notebook is posted at [https://nbviewer.org/url/relativite.obspm.fr/notebooks/BH\\_3D\\_supergravity.ipynb](https://nbviewer.org/url/relativite.obspm.fr/notebooks/BH_3D_supergravity.ipynb)

## 2 Setup

### 2.1 The holographic model

The action of the 3D truncated supergravity reads

$$S = \frac{1}{16\pi G_3} \int d^3x \sqrt{|g|} \left( R - \frac{1}{a^2} (\partial\phi)^2 - V(\phi) \right) + \frac{1}{8\pi G_3} \int_{\partial M} d^2x \sqrt{|\gamma|} K, \quad (2.1)$$

with the potential  $V(\phi)$  is given by:

$$V(\phi) = 2\Lambda_{\text{uv}} \cosh^2 \phi \left[ (1 - 2a^2) \cosh^2 \phi + 2a^2 \right], \quad (2.2)$$

where the parameter  $a$  is non-zero and is related to the curvature of the target manifold. In what follows we focus on the cases: **a)**  $a^2 \leq \frac{1}{2}$  and **b)**  $\frac{1}{2} \leq a^2 \leq 1$ .

The Gibbons-Hawking-York (GHY) boundary term in (2.1) includes the determinant of the induced metric  $\gamma$  on the boundary  $\partial M$  and the extrinsic curvature  $K$

$$K = \gamma^{\mu\nu} K_{\mu\nu}, \quad K_{\mu\nu} = -\nabla_\mu n_\nu = \frac{1}{2} n^\rho \partial_\rho \gamma_{\mu\nu}, \quad n^\mu = \frac{\delta_w^\mu}{\sqrt{g_{ww}}}. \quad (2.3)$$

We show the behaviour of the potential on the scalar field in Fig. 1. Note that for  $a^2 \leq \frac{1}{2}$  and for  $a^2 \geq 1$  the potential has one extremum, namely,

$$\phi_1 = 0, \quad (2.4)$$

while for  $\frac{1}{2} < a^2 < 1$  the potential has two more extremal points, i.e.

$$\phi_{2,3} = \frac{1}{2} \ln \left( \frac{1 \pm 2|a|\sqrt{1-a^2}}{2a^2-1} \right). \quad (2.5)$$

Moreover, if we consider the case  $a^2 > \frac{1}{2}$  the scalar potential has also zeroes:

$$\phi_{\pm} = \pm \cosh^{-1} \left( \frac{a}{\sqrt{a^2 - \frac{1}{2}}} \right). \quad (2.6)$$

The behavior of the potential  $V$  on  $\phi$  for various  $a$  is presented in Figs. 1. We marked by  $\phi_3$  and  $\phi_2$  (2.5) the left and right extrema of the potential, correspondingly.

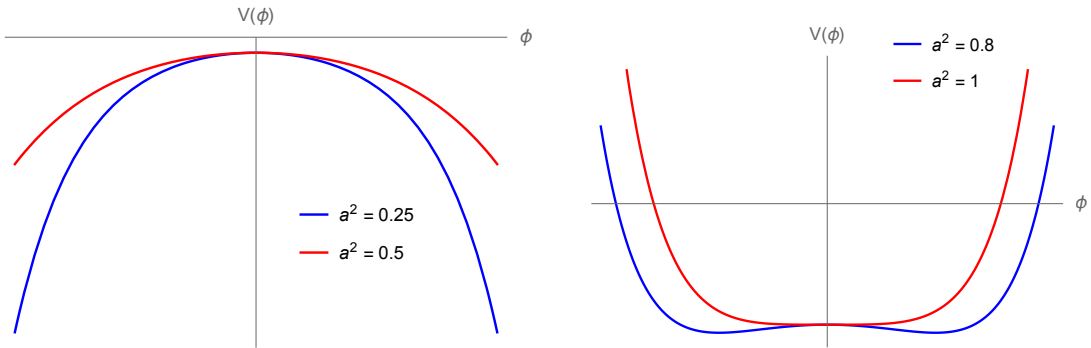


Figure 1: The potential (2.2) against the scalar field  $\phi$  for different values of  $a$ . For all we set  $\Lambda_{\text{uv}} = -1$ .

We focus on holographic RG flows at finite temperature for the model (2.1) for these reasons we consider the following ansatz of the metric in the domain wall coordinates

$$ds^2 = e^{2A(w)} \left( -f(w)dt^2 + dx^2 \right) + \frac{dw^2}{f(w)}, \quad (2.7)$$

with the radial coordinate running the region  $w \in (w_h, +\infty)$ , such that  $w_h$  is a position of the horizon and the conformal boundary is located at  $w \rightarrow +\infty$ . In (2.7) the scale factor  $A = A(w)$ , the function and  $f(w)$  defines the position of the horizon, such that it has the following structure

$$\begin{cases} f < 0, & \text{for } w < w_h, \\ f = 0, & \text{for } w = w_h, \\ f > 0, & \text{for } w > w_h, \end{cases} \quad (2.8)$$

and  $f = 1$  on the boundary of the spacetime. The temperature of the solution (2.7) can be found as [18]

$$T_H = \frac{e^{A(w_h)}}{4\pi} \left. \frac{df}{dw} \right|_{w=w_h}. \quad (2.9)$$

The Hawking temperature (2.9) of the black hole (2.7) corresponds to the temperature of the dual field theory.

The entropy density of the solution is given by

$$s = 4\pi M_p e^{A(w_h)}, \quad (2.10)$$

with

$$M_p = \frac{1}{16\pi G_3}. \quad (2.11)$$

The scalar field profile has the dependence only on the radial coordinate  $w$

$$\phi = \phi(w). \quad (2.12)$$

We are looking for black hole solutions with the metric (2.7) such that the scalar field has some finite value at the horizon  $w_h$

$$\phi(w_h) = \phi_h. \quad (2.13)$$

In what follows it is convenient to introduce the function

$$g = \ln f. \quad (2.14)$$

Then the Einstein equations to (2.1) can be represented in the following form

$$\ddot{A} + \frac{\dot{\phi}^2}{a^2} = 0, \quad (2.15)$$

$$\ddot{g} + \dot{g}^2 + 2\dot{g}\dot{A} = 0, \quad (2.16)$$

$$\dot{A}\dot{g} + 2\dot{A}^2 - \frac{\dot{\phi}^2}{a^2} + e^{-g}V = 0, \quad (2.17)$$

where the overdot indicates the derivative with respect the radial coordinate  $w$ . The scalar field equation is

$$\ddot{\phi} + \dot{g}\dot{\phi} + 2\dot{A}\dot{\phi} - \frac{a^2}{2}e^{-g}V_\phi = 0, \quad (2.18)$$

where  $V_\phi$  is a derivative of the potential with respect to  $\phi$ .

Note, that for  $f = 1$  the model has an exact half-supersymmetric solution, which interpolates between AdS and scaling geometries [27].

## 2.2 The dynamical system in $\mathbf{R}^3$

We are looking black hole solutions (2.7) with (2.13) to (2.1), which can be interpreted as holographic RG flows at finite temperature. For this, we represent eqs.(2.15)-(2.18) as an autonomous dynamical system introducing new variables [14, 17]

$$X = \frac{d\phi}{dA} = \frac{\dot{\phi}}{\dot{A}}, \quad Y = \frac{dg}{dA} = \frac{\dot{g}}{\dot{A}}, \quad (2.19)$$

where  $g = \ln f$ ,  $\phi$  is the dilaton,  $A$  is the scale factor, and the derivatives are taken with respect to the radial coordinate  $w$ . So both variables  $X$  and  $Y$  run from  $-\infty$  to  $\infty$ . In [18] it was shown that the first order formalisms for the holographic RG flows in terms of the the variables  $X, Y$  and the superpotential are equivalent.

As for the scalar field it is convenient to compactify it using the following redefinition:

$$z = \frac{1}{1 + e^\phi}, \quad (2.20)$$

so that  $z \in [0, 1]$  for  $\phi \in (-\infty; \infty)$ . Below we will use (2.5) and (2.6) as  $z_i = z(\phi_i)$  with  $i = 1, 2, 3$  and  $z_\pm = z(\phi_\pm)$ .

The ratio of the potential and its derivative in terms of the variable  $z$  (2.20) is represented as follows

$$\frac{V_\phi}{V} = -\frac{4(4a^2z^4 - 8a^2z^3 + 12a^2z^2 - 4z^4 - 8a^2z + 8z^3 + 2a^2 - 8z^2 + 4z - 1)(2z - 1)}{(8a^2z^2 - 4z^4 - 8a^2z + 8z^3 + 2a^2 - 8z^2 + 4z - 1)(2z^2 - 2z + 1)}. \quad (2.21)$$

Taking into account (2.19)-(2.20) the equations of motion (2.15)-(2.18) are brought to

$$\frac{dz}{dA} = z(z - 1)X, \quad (2.22)$$

$$\frac{dX}{dA} = \left( \frac{X^2}{a^2} - Y - 2 \right) \left( X + \frac{a^2}{2} \frac{V_\phi}{V} \right), \quad (2.23)$$

$$\frac{dY}{dA} = Y \left( \frac{X^2}{a^2} - Y - 2 \right), \quad (2.24)$$

where in (2.23) we also suppose (2.21).

The equilibrium points of the dynamical system (2.22)-(2.24) can be related with the fixed points of holographic RG flows. It worth to be noted that the critical points with  $Y = 0$  correspond to zero-temperature regime. Thus, the conformal boundary of the black hole spacetime corresponds to  $Y \rightarrow 0$ , while at the horizon  $Y$  tends to infinity  $Y \rightarrow \infty$ .

## 2.3 The dynamical system in the cylinder

To understand the behaviour of flows at infinity we apply the so-called Poincaré projection [36], which maps the system into the unit cylinder. We use Poincaré projection only over the variables  $X$  and  $Y$  due to  $z$  is compact.

To extract the information about the finite temperature flows we map the system (2.23)-(2.24) defined on the plane  $\mathbf{R}^2$  into the disc  $\mathbf{D}^2$ . This allows to consider infinite points of eqs.(2.23)-(2.24), which are difficult to be caught considering the system on  $\mathbf{R}^2$ .

The coordinates of the system on  $\mathbf{R}^2$  are related with the coordinates on  $\mathbf{D}^2$  by

$$X = \frac{x}{\sqrt{1-x^2-y^2}}, \quad Y = \frac{y}{\sqrt{1-x^2-y^2}}. \quad (2.25)$$

For the new coordinates  $x, y$  on  $\mathbf{D}^2$  we also have the constraint

$$x^2 + y^2 \leq 1. \quad (2.26)$$

Applying the coordinate transformations (2.25) for  $X$  and  $Y$  to eqs. (2.22)-(2.24), we come to the dynamical system in the  $3d$  unit cylinder

$$z' = z(z-1)x, \quad (2.27)$$

$$x' = p(x, y, z), \quad (2.28)$$

$$y' = q(x, y, z), \quad (2.29)$$

where  $p, q$  are represented by

$$\begin{aligned} p &= \left( \sqrt{1-x^2-y^2} \left( 2\sqrt{1-x^2-y^2} + y \right) - \frac{x^2}{a^2} \right) \left( \frac{a^2 V_\phi}{2V} (x^2 - 1) - x\sqrt{1-x^2-y^2} \right), \\ q &= \left( \sqrt{1-x^2-y^2} \left( 2\sqrt{1-x^2-y^2} + y \right) - \frac{x^2}{a^2} \right) \left( \frac{a^2 V_\phi}{2V} x - \sqrt{1-x^2-y^2} \right) y \end{aligned} \quad (2.30)$$

and the derivatives are redefined as

$$\chi' = \sqrt{1-x^2-y^2} d\chi/dA. \quad (2.31)$$

This is admissible, since, such redefinition does preserves the behavior of flows, and at the same time allows us to avoid divergences, which arise for  $x^2 + y^2 = 1$ .

The dynamical system (2.27)-(2.29) with (2.30) has a rich structure of equilibrium sets, that was investigated in [28]. We omit the discussion of this issue here, keeping in mind only, that the equilibrium points  $p_i$  have the coordinates  $(0, 0, z_i)$ , where  $z_i$  takes the value at the  $i$ -extremum, and correspond to the AdS spacetimes, while the points  $\bar{p}_i$  are related with the near-horizon regions and have the coordinates  $(0, 1, z_i)$ .

The asymptotically AdS black hole solutions to eqs.(2.27)-(2.29) were found numerically in [28], such that for  $a^2 \leq \frac{1}{2}$  we used the following initial conditions

$$x = 0, \quad y = 1 - \varepsilon, \quad z \in (0, 1), \quad (2.32)$$



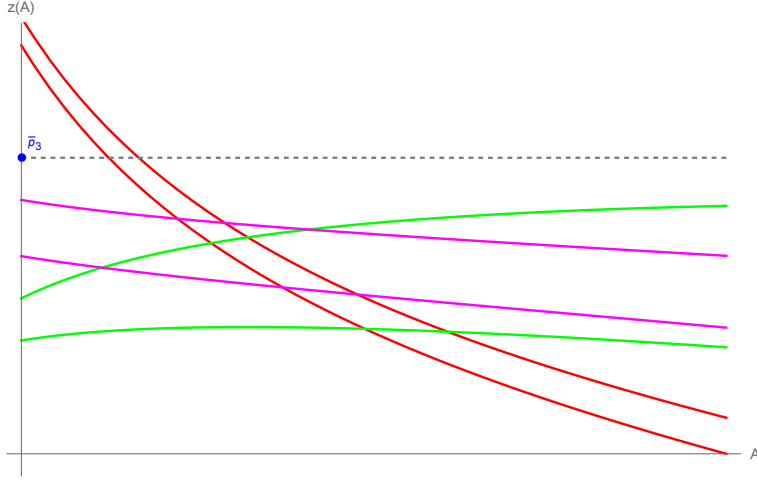


Figure 2: Three different types of numerical trajectories near the horizon for the component  $z(A)$  of the dynamical system (2.22)-(2.24) with initial conditions (2.34),  $a^2 = 0.8$ . All trajectories correspond to the asymptotically AdS black holes in the near-horizon region. For red:  $v > 0$ ,  $\delta > 0$ . For magenta:  $v < 0$ ,  $\delta < 0$ . For green (non-monotonic):  $v > 0$ ,  $\delta < 0$ . The dark grey dashed line is the exact AdS black hole solution (3.1)-(3.2) with  $\phi_h = \phi_3$ .

i.e. the value of the scalar field on the horizon  $\phi_h$  can take any value of the range of the potential, the initial value of  $y$  should be close to the near horizon region and, finally,  $x$  and  $y$  should respect (2.26). For the case  $\frac{1}{2} < a^2 < 1$  the initial conditions are slightly modified such that  $\phi_h$  runs either in the interval  $(\phi_2, \phi_1)$  or  $(\phi_1, \phi_3)$ , i.e.

$$x = 0, \quad y = 1 - \varepsilon, \quad z \in [z_2 + \delta, z_3 - \delta], \quad (2.33)$$

where  $\delta > 0$ . For  $\frac{1}{2} < a^2 < 1$  there is a broader class of asymptotically AdS black hole solutions with the initial conditions given by

$$x = v, \quad y = 1 - \varepsilon, \quad z \in [z_2 - \delta, z_3 + \delta], \quad (2.34)$$

with  $v \neq 0$ , such that for  $\phi_h \in (\phi_3, \phi_3 + \delta)$  the parameter  $v$  is positive and for  $\phi_h \in (\phi_2, \phi_2 - \delta)$  the  $v$  is negative. The dynamics of the solutions with (2.32), (2.33) and (2.34) was analyzed in [28]. Note, that the some solutions with the initial conditions (2.34) have a non-monotonic behaviour of  $\phi$  comparing to those with (2.32) or (2.33). In Fig. 2 we plot  $z$  of the numerical black hole solutions as a function of  $A$  with the initial conditions (2.34) for the case of three extrema of the potential with  $a^2 = 0.8$ . We show the behaviour of the solutions in the near-horizon region. The trajectories start near the point  $\bar{p}_3$ , which is related with  $\phi_3$ , and end in  $p_1$  corresponding to  $\phi_1$ .

Below we will present analytic description of black hole solutions, which are related with (2.32) and (2.33), and discuss its thermodynamical properties.

### 3 Asymptotically AdS (BTZ) black hole solutions

#### 3.1 Exact BTZ black holes

AdS black holes (non-rotating BTZ solution) can be obtained as a solution of the autonomous system. It corresponds to  $X = 0$  and  $Z = \text{const}$  in (2.19)-(2.20) and  $\phi_h = \phi_i$ ,  $i = 1, 2, 3$ . The metric of the 3d AdS black hole in the domain wall coordinates reads

$$ds^2 = e^{2A} \left( -f(w)dt^2 + dx^2 \right) + \frac{dw^2}{f(w)}, \quad (3.1)$$

where

$$A = \sqrt{-\frac{V(\phi_h)}{2}}w, \quad f = 1 - e^{-\sqrt{-2V(\phi_h)}(w-w_h)}. \quad (3.2)$$

The boundary of the spacetime is reached as  $w \rightarrow \infty$  and the horizon  $w \rightarrow w_h$ .

Setting  $x = \varphi$  with  $\varphi \in [0, 2\pi)$ , the metric (3.1)-(3.2) takes a standard form of the non-rotating BTZ black hole [37].

The temperature and the entropy of the BTZ black hole solution are

$$T_H = \frac{1}{2\pi\ell} e^{w_h/\ell}, \quad s = 4\pi M_p e^{w_h/\ell}. \quad (3.3)$$

In the near-horizon region the metric functions takes the form (3.1)

$$A|_{w \rightarrow w_h} \simeq \sqrt{-\frac{V(\phi_h)}{2}}w_h, \quad f|_{w \rightarrow w_h} = \sqrt{-2V(\phi_h)}(w - w_h) + \dots \quad (3.4)$$

#### 3.2 Near-horizon asymptotically AdS black holes

In [28] it was shown that the equation for the variable  $Y$  of the system (2.22)-(2.24) can be split off for the near-horizon region with  $Y \rightarrow \infty$  and easily integrated

$$Y = \frac{1}{A - A_h}, \quad (3.5)$$

where  $A_h = A(w_h)$ . Now it is convenient to find a solution for  $\phi$  in terms of  $A$  and then find  $A$ . The other two equations can be represented as a single second order equation for  $\phi$

$$(A - A_h) \frac{d^2\phi}{dA^2} + \frac{d\phi}{dA} + \frac{a^2 V_\phi(\phi)}{2 V(\phi)} = 0. \quad (3.6)$$

To proceed we expand the term  $\frac{V_\phi(\phi)}{V(\phi)}$  in Taylor series near  $\phi_h$

$$\left. \frac{a^2 V_\phi(\phi)}{2 V(\phi)} \right|_{\phi_h} = \Lambda^{(h)} + \mathbf{K}^{(h)}(\phi - \phi_h), \quad (3.7)$$

where we denote

$$\Lambda^{(h)} = \frac{a^2 V_\phi(\phi_h)}{2 V(\phi_h)}, \quad \Delta^{(h)} = \frac{a^2 V_{\phi\phi}(\phi_h)}{2 V(\phi_h)}, \quad \mathbf{K}^{(h)} = \left( \Delta^{(h)} - \frac{2}{a^2} (\Lambda^{(h)})^2 \right). \quad (3.8)$$

Note, that for  $a^2 \leq \frac{1}{2}$  the quantity  $\mathbf{K}^{(h)}$  is always non-negative, while for  $\frac{1}{2} < a^2 < 1$  we have to trace the sign of  $\mathbf{K}^{(h)}$  with respect to the position of  $\phi_h$  and also take into account zeros of the scalar potential.

The solution to eq. (3.6) with (3.7) near  $A_h$  can be represented as follows

$$\phi(A) = \phi_h - \Lambda^{(h)}(A - A_h), \quad (3.9)$$

with  $\Lambda^{(h)}$  given by (3.8). Note that the solution (3.9) corresponds to the following initial conditions

$$\phi(A_h) = \phi_h, \quad \phi'(A_h) = -\Lambda^{(h)}. \quad (3.10)$$

Subtracting (2.15) from (2.17) we come the equation

$$\ddot{A} + \dot{A}^2 \left( \frac{d\phi(A)}{dA} \right)^2 = 0. \quad (3.11)$$

Taking into account (3.9), we find a solution for the scale factor

$$A(w) = \frac{a^2}{(\Lambda^{(h)})^2} \ln \left( \frac{\frac{(\Lambda^{(h)})^2}{a^2} w + c_A}{c_A} \right), \quad (3.12)$$

with

$$c_A = \sqrt{-\frac{2}{V(\phi_h)}}, \quad (3.13)$$

where the constants of integration are chosen such that (3.12) matches with the near-horizon AdS black hole solution if  $\phi_h$  is the critical point of the potential.

The blackening function  $f$  near the horizon us

$$f = e^{c_g}(A - A_h), \quad (3.14)$$

with the integration constant  $c_g$ , which reads from the which is found from the Einstein equations as follows

$$c_g = \ln \left( |V(\phi_h)| \left( c_A + \frac{(\Lambda^{(h)})^2}{a^2} w_h \right)^2 \right). \quad (3.15)$$

Introducing the quantity

$$\kappa = \frac{(\Lambda^{(h)})^2}{a^2}, \quad (3.16)$$

where the parameter  $\Lambda^{(h)}$  is given by (3.8), the black hole metric can be represented as follows

$$ds^2 \simeq \left( 1 + \frac{\kappa}{c_A} w \right)^{2/\kappa} \left( -f dt^2 + dx^2 \right) + \frac{dw^2}{f}, \quad (3.17)$$

with the blackening function (3.14) reads as

$$f = \frac{e^{c_g}}{\kappa} \ln \left( \frac{1 + \frac{\kappa}{c_A} w}{1 + \frac{\kappa}{c_A} w_h} \right) \quad (3.18)$$

with  $c_A$  defined by (3.13) and  $c_g$  (3.15) represented as

$$c_g = \ln \left( 2 \left( 1 + \frac{\kappa}{c_A} w_h \right)^2 \right). \quad (3.19)$$

From the latter one can see that for  $\phi_h = \phi_{1,2,3}$ ,  $c_g$  turns to be  $c_g = \ln 2$  as for the near-horizon metric of the AdS black hole.

The scalar field of the solution (3.9) is non-zero and given by

$$\phi(A) = \phi_h - \frac{\Lambda^{(h)}}{\kappa} \ln \left( \frac{1 + \frac{\kappa}{c_A} w}{1 + \frac{\kappa}{c_A} w_h} \right). \quad (3.20)$$

For vanishing  $\Lambda^{(h)}$ , corresponding to extrema of the potential  $V_\phi = 0$ , the near-horizon solution turns to be the BTZ black hole with a constant scalar field and near-horizon metric functions (3.4).

### 3.3 Thermodynamics of the near-horizon solutions

Here we discuss the thermodynamics of the black hole solutions, which we constructed in the previous section. We note, that in the case of one extremum of the potential,  $a^2 \leq \frac{1}{2}$ , the value of the scalar field at the horizon  $\phi_h$  can take any value on the range of  $V$ . For the case of the potential with three extrema,  $\frac{1}{2} < a^2 < 1$  we are restricted as  $\phi_h \in (\phi_2, \phi_3)$ .

The Hawking temperature of the black hole solution (3.17) with (3.18) and (3.20) can be calculated using (2.9). Then the temperature reads

$$T_H = \frac{1}{2\pi c_A} \mathbf{B}^{\frac{\kappa+1}{\kappa}}, \quad (3.21)$$

where we introduced the quantity

$$\mathbf{B} = 1 + \frac{\kappa}{c_A} w_h, \quad (3.22)$$

where  $c_A$  is given by (3.13) and  $\kappa$  by (3.16). We present the behaviour of the temperature as a function of the value of the scalar field on the horizon  $\phi_h$  in Fig. 3 for  $a^2 = 0.25$  and  $a^2 = 0.8$  with fixed  $w_h$ . The temperature symmetrically increases for opposite values of  $\phi_h$ , for  $a^2 = 0.8$  the temperature is bounded by a maximal value due to the restriction for the value of  $\phi_h$ . At the extrema of the potentials, that corresponds to  $\kappa \rightarrow 0$  (3.16), the thermodynamics becomes conformal and the temperature is given by (3.3) for both cases of  $a^2$ . This can be checked

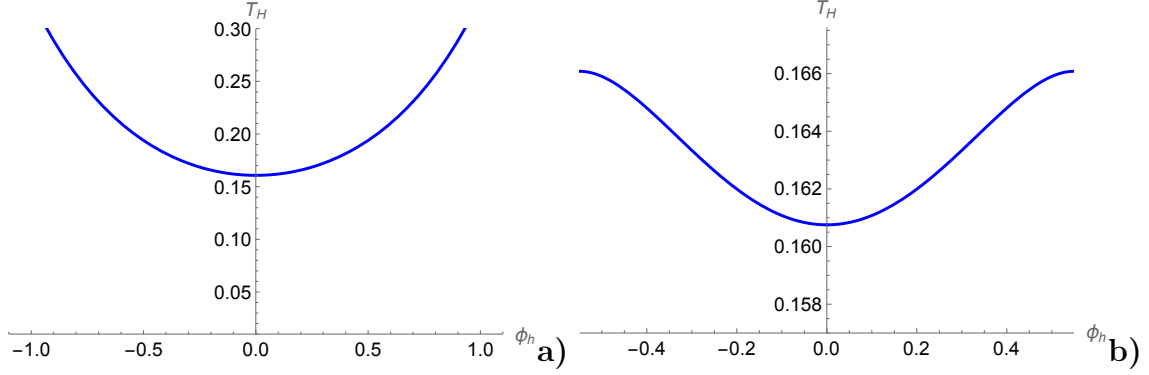


Figure 3: Hawking temperature (3.21) as a function of  $\phi_h$ : a)  $a^2 = 0.25$ , b)  $a^2 = 0.8$ ; for all we set  $w_h = 0.01$ .

expanding in series (3.21) by small  $\Lambda^{(h)}$ . Thus, near the extremum of the potential  $V$  with  $\Lambda^{(h)} \simeq 0$  the temperature reads

$$T_{H,\Lambda^{(h)} \rightarrow 0} = \frac{e^{w_h/c_A}}{2\pi c_A} + \frac{e^{w_h/c_A}(2c_A - w_h)w_h(\Lambda^{(h)})^2}{4\pi a^2 c_A^3}. \quad (3.23)$$

Using (2.10) one finds that the entropy of the black hole solution (3.17) with (3.18) is given by

$$s = 4\pi M_p \mathbf{B}^{\frac{1}{\kappa}}. \quad (3.24)$$

We show the behavior of the entropy (3.24) as a function of  $\phi_h$  in Fig. 4. One can see that for  $a^2 = 0.8$  the entropy has its maximal value comparing to the case  $a^2 = 0.25$ , for which the entropy is unbounded from above. Again, if  $\phi_h$  matches with the value at extremum the entropy is given by (3.3).

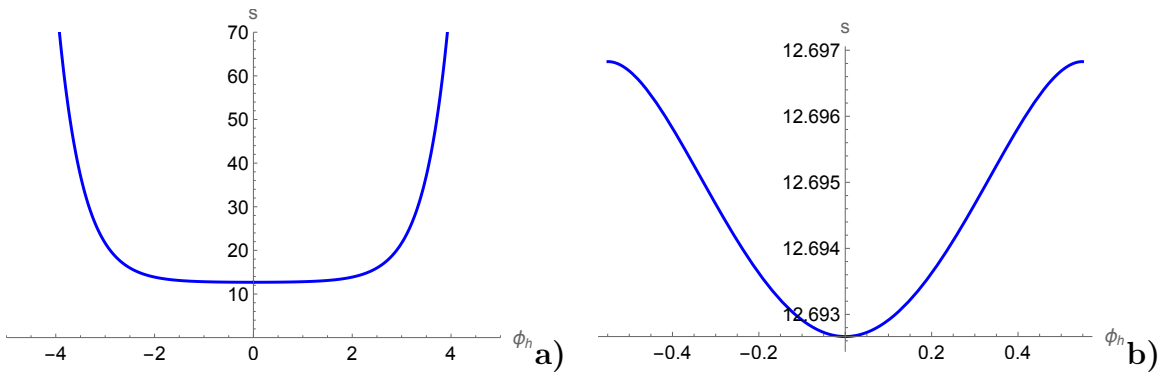


Figure 4: Entropy density (3.24) as a function of  $\phi_h$ : a)  $a^2 = 0.25$ , b)  $a^2 = 0.8$ ; for all we set  $w_h = 0.01$ .

We show the behaviour of the entropy  $s$  (3.24) as a function of  $T_H$  (3.21) in Fig. 5.

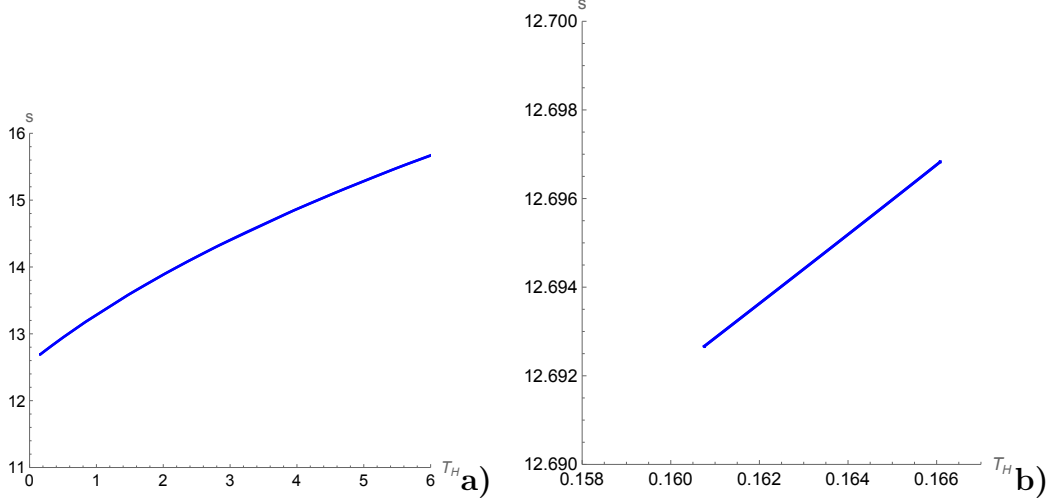


Figure 5: Entropy density (3.24) vs Hawking temperature (3.21) for a)  $a^2 = 0.25$ , b)  $a^2 = 0.8$ ; for all we set  $w_h = 0.01$  .

It is useful to look on the product of the temperature and the entropy

$$sT_H = \frac{2M_p}{c_A} \left(1 + \frac{\kappa}{c_A} w_h\right)^{\frac{2+\kappa}{\kappa}} = \frac{2M_p}{c_A} \mathbf{B}^{\frac{2+\kappa}{\kappa}}. \quad (3.25)$$

Taking into account (3.21),(3.24) and (3.25) the free energy can be found as follows

$$\mathcal{F} = - \int s dT_H = - \frac{2M_p}{c_A} \int_1^{\mathbf{B}} \frac{\bar{\mathbf{B}}^{\frac{2+\kappa}{\kappa}}}{T_H} \frac{dT_H}{d\bar{\mathbf{B}}} d\bar{\mathbf{B}} = - \frac{2M_p}{c_A} \frac{\kappa + 1}{\kappa + 2} \left(\mathbf{B}^{1+\frac{2}{\kappa}} - 1\right). \quad (3.26)$$

For  $\phi_h = \phi_1$  the thermodynamics is conformal, that can be seen from the expansion of the free energy with  $\Lambda^{(h)} \simeq 0$

$$\mathcal{F}_{\Lambda^{(h)} \rightarrow 0} = - \frac{e^{\frac{2w_h}{c_A}}}{c_A} - \frac{e^{\frac{2w_h}{c_A}} (c_A^2 - 2w_h^2 + 2c_A w_h)}{2a^2 c_A^3} (\Lambda^{(h)})^2, \quad (3.27)$$

i.e. from (3.23) and (3.27) we get as expected

$$\mathcal{F} \sim T^d, \quad (3.28)$$

where  $d = 2$ . In Fig. 6 we show the dependence of  $\mathcal{F}$  on  $T_H$ .

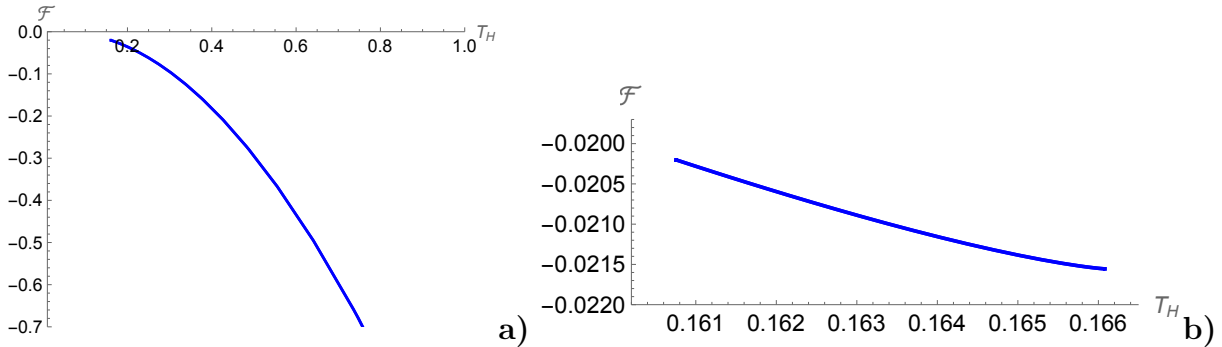


Figure 6: Free energy (3.26) as a function of Hawking temperature (3.21) for a)  $a^2 = 0.25$ , b)  $a^2 = 0.8$ ; for all we set  $w_h = 0.01$

## 4 From the near-horizon region to the boundary

### 4.1 Analytic solutions from the horizon to the boundary

In this section we will discuss analytic asymptotically AdS black hole solutions, defined for both near the horizon and near the boundary regions. These solutions can be obtained using an additional condition

$$X^2 \sim 0, \quad (4.1)$$

the validity of using which we observed from the behaviour of numerical holographic RG flows of the system (2.22)-(2.24). In fact, the constraint (4.1) says about the slowly changing scalar field. Below we will show that the constraint (4.1) allows to reduce the dynamical system such that the equation for the variable  $Y$  decouples and the equations for the scalar field and the scale factor are simplified.

Thus, imposing the constraint (4.1) for eqs. (2.22)-(2.24) we come to the system of equations

$$\frac{dz}{dA} = z(z-1)X, \quad (4.2)$$

$$\frac{dX}{dA} = -(Y+2) \left( X + \frac{a^2 V_\phi}{2V} \right), \quad (4.3)$$

$$\frac{dY}{dA} = -Y(Y+2). \quad (4.4)$$

Mapping the system (4.2)-(4.4) into a unit cylinder, one can find that for the case  $0 < a^2 < 1/2$  the numerical solutions with the condition (4.1) from the near-horizon region with some  $\phi_h$  to the AdS critical point  $p_1$  have a greater deviation from the numerical trajectories of the system (2.27)-(2.29) without additional constraints ending in  $p_1$ , the further the initial condition for  $\phi_h$  from the extremum  $\phi = 0$  ( $z = 1/2$ ) is chosen. In Fig. 7 we show the trajectories of (4.2)-(4.4) in the cylinder for  $0 < a^2 \leq 1/2$ . The solid curves correspond to the holographic

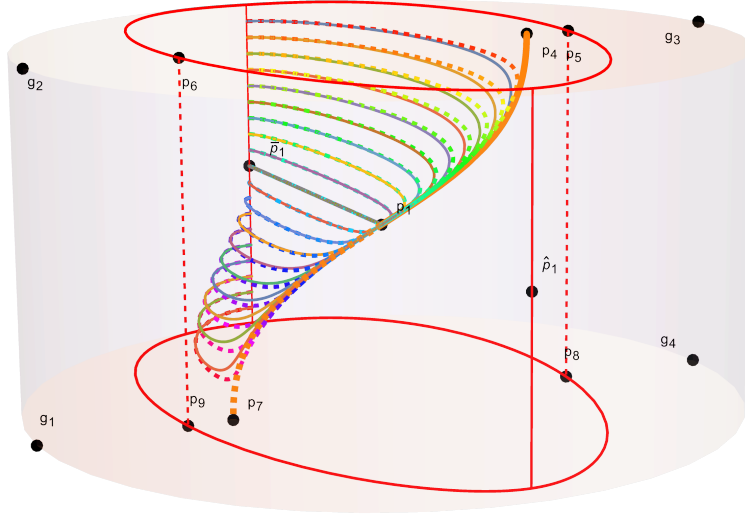


Figure 7: The numerical trajectories of the dynamical systems (2.22)-(2.24) and (4.2)-(4.4) (dashed) in the cylinder for  $a^2 = 0.25$ .

RG flows of (2.27)-(2.29) without additional constraints, while the dashed curves are numerical solutions with the condition (4.1).

To find the analytical form of the solutions to (4.2)-(4.4), we assume that the variable  $Y$  tends to infinity near the horizon,  $Y(0) \rightarrow \infty$ . The equation (4.4) is independent and can be easily integrated as

$$Y(A) = \frac{2}{e^{2(A-A_h)} - 1}. \quad (4.5)$$

Plugging (4.5) into eq.(4.3) and returning from  $z$  to the original variable  $\phi$  (2.20) the other two equations can be represented as a single second-order differential equation for the scalar field  $\phi$  on  $A$

$$\frac{d^2\phi}{d(A-A_h)^2} + (1 + \coth(A-A_h)) \left( \frac{d\phi}{d(A-A_h)} + \frac{a^2 V_\phi(\phi)}{2 V(\phi)} \right) = 0. \quad (4.6)$$

We note that the equation (4.6) is not expanded near the horizon, i.e. a Taylor series expansion of (4.6) by  $A$  near  $A_h$  up to the first order yields the scalar field equation (3.6). However, we note the expansion of the potential term in (4.6) can be done if  $\phi_h$  is taken near  $\phi_1$  both for  $a^2 < \frac{1}{2}$  and  $\frac{1}{2} < a^2 < 1$ . The scalar field corresponding to the trajectories starting from  $\phi_{2,3}$  ( $\bar{p}_{2,3}$ ), as well as for  $\phi_h$  far from  $\phi_1$ , changes fast [28] that precludes to use the expansion of  $\frac{V_\phi}{V}$ . Thus, we are able to construct the trajectories with the constraint (4.1) from  $\bar{p}_{2,3}$  to  $p_1$  numerically, but we cannot succeed analytically.

Eq.(4.6) near  $\phi_h$  can be brought to the hypergeometric equation

$$r(1-r) \frac{d^2\Phi(r)}{dr^2} + (1-2r) \frac{d\Phi(r)}{dr} - \frac{K^{(h)}}{2} \Phi(r) = 0, \quad (4.7)$$



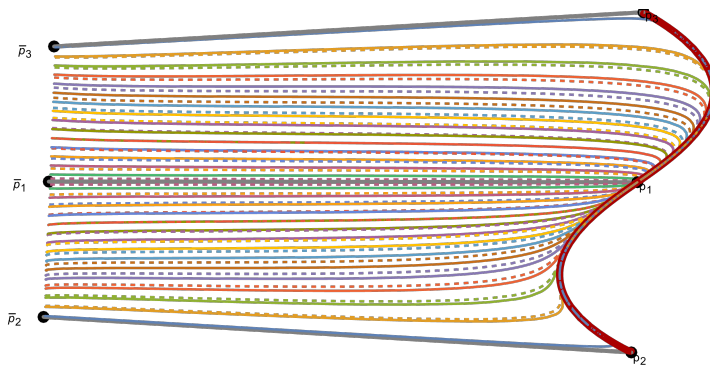


Figure 8: The numerical trajectories of the dynamical systems (2.22)-(2.24) (solid) and (4.2)-(4.4) (dashed) for  $a^2 = 0.8$ . The values of  $\phi_h$  for the dashed flows corresponding to (4.2)-(4.4) slightly differ from the initial conditions for (2.22)-(2.24), otherwise they would completely merge in the figure.

where we define

$$\Phi := \phi - \phi_h + \frac{\Lambda^{(h)}}{\mathcal{K}^{(h)}}, \quad (4.8)$$

with  $\Lambda^{(h)}$  and  $\mathcal{K}^{(h)}$  given by (3.8) and

$$r = \exp 2(A - A_h). \quad (4.9)$$

It is worth to be noted that we can derive eq.(4.7) from EOM for the scalar field (2.18) under the assumption (4.1), which it turn says that  $A$  is linear.

The regular singular points  $r = 1$  and  $r = \infty$  of eq.(4.7) correspond to the near-horizon and boundary regions, respectively.

Then, the solution for the scalar field near the horizon can be read off immediately from the fundamental solution to eq. (4.7) near  $r = 1$ , namely,

$$\Phi(r) = {}_2F_1(a_h, 1 - a_h, 1, 1 - r), \quad (4.10)$$

where  $a_h$  is

$$a_h = \frac{1}{2} \left( 1 - \sqrt{1 - 2\mathcal{K}^{(h)}} \right). \quad (4.11)$$

The solution (4.10) is divergent at  $r = 0$ , which is not of our interest, but finite in the region from  $r = 1$  to  $r = \infty$ . We show the behaviour of the solution (4.10) in Fig. 9 b) for  $a^2 = 0.25$  (solid) and  $a^2 = 0.8$  (dashed).

As for the metric function  $A$ , the constraint (4.1) leads to the fact that the equations of motion (2.15)-(2.17) are simplified and we have for  $A$

$$\ddot{A} = 0. \quad (4.12)$$

Then, the solution to (4.12) is given by

$$A = \mathbf{c}_A w + \mathbf{c}_2, \quad (4.13)$$

where the constants of integration are chosen as

$$\mathbf{c}_A = \sqrt{-\frac{V(\phi_h)}{2}}, \quad \mathbf{c}_2 = 0. \quad (4.14)$$

The blackness function  $f$  can be found from (4.5) and the definition of  $Y$  (2.19)

$$f = e^{c_g} \left(1 - e^{-2\mathbf{c}_A(w-w_h)}\right), \quad (4.15)$$

so the constant  $c_g$  should be fixed from the equations of motion (2.15)-(2.17) as  $c_g = 0$ .

Taking into account (4.13)-(4.14) the solution for the scalar field takes the form

$$\phi = \phi_h + {}_2F_1 \left( \frac{1 - \sqrt{1 - 2\Delta^{(h)}}}{2}, \frac{1 + \sqrt{1 - 2\Delta^{(h)}}}{2}, 1, 1 - e^{\mathbf{c}_A(w-w_h)} \right). \quad (4.16)$$

It is interesting to note that the constraint (4.1) brings us that the metric of the solution matches with the metric of the non-rotating BTZ black hole (3.1)-(3.2), while the scalar field is a solution to the hypergeometric equation (4.7). This equation appears if one considers merely a scalar field in the BTZ black hole background. So this class of the solutions has a conformal thermodynamics. It worth also to be noted that in [32] it was shown that constraint (4.1) is related with the condition for vanishing of the  $c$ -function.

## 4.2 The behaviour of the scalar field near boundary

Despite the solution for the scalar field (4.10) is obtained for the region near the horizon, from Fig. 7 we can observe that such flows end in the AdS critical point  $p_1$ , if the value of the scalar field on the horizon is taken in the neighbourhood of the extremum  $\phi = 0$ . This happens because the hypergeometric function (4.10) can be extended from the region  $r = 1$  to  $r \rightarrow +\infty$ .

Consider the behavior of the scalar field (4.8) with (4.10) near the boundary  $r \rightarrow \infty$ , taking into account  $\Lambda^{(h)} \sim 0$ . The Taylor series expansion of (4.10) near the boundary  $r \rightarrow +\infty$  leads to

$$\phi_{A \rightarrow \infty} \simeq \frac{\Gamma(\Delta_- - 1)}{\Gamma(\frac{\Delta_-}{2})^2} e^{-\Delta_+ w/\ell} + \dots + \frac{\Gamma(\Delta_+ - 1)}{\Gamma(\frac{\Delta_+}{2})^2} e^{-\Delta_- w/\ell} + \dots, \quad (4.17)$$

where we used that near  $\phi_h = 0$  the integration constant  $\mathbf{c}_A$  (4.14) can be related with the radius of the AdS spacetime in  $\phi = 0$

$$\mathbf{c}_A = 1/\ell. \quad (4.18)$$

The conformal dimensions  $\Delta_{\pm}$  of the dual operator are defined by

$$\Delta_{\pm} = 1 \pm \sqrt{1 + M^2 \ell^2} = 1 \pm \sqrt{1 + \frac{a^2}{2} V_{\phi\phi}(\phi_1) \ell^2}, \quad (4.19)$$

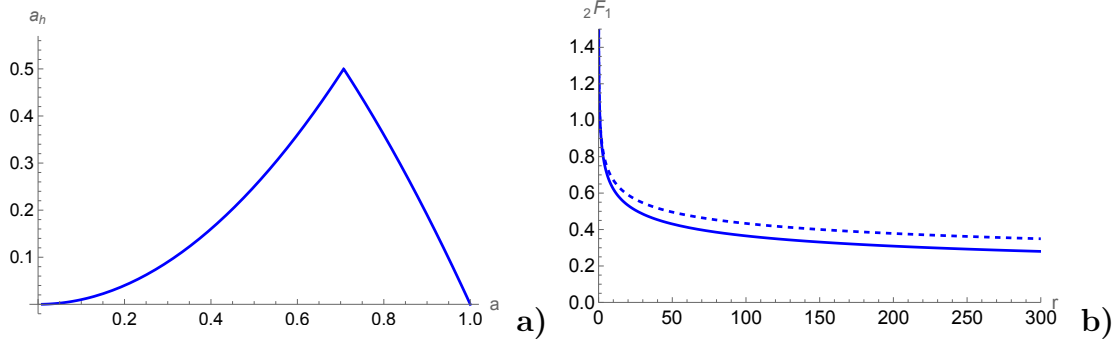


Figure 9: **a)** The dependence of the parameter  $a_h$  (4.11) on  $a$ ; **b)** The behaviour of  ${}_2F_1(a_h, 1 - a_h, 1, 1 - r)$  on  $r$  for  $a^2 = 0.25$  (solid),  $a^2 = 0.8$  (dashed).

with  $M^2 = V_{\phi\phi}(\phi_1)$ , i.e. we used

$$1 \pm \sqrt{1 - 2\Delta^{(h)}} = 1 \pm \sqrt{1 + M_\phi^2 \ell^2}. \quad (4.20)$$

Moreover, the coefficients in (4.17) coincide with those from [38]. The form (4.17) matches with the statement that the scalar field near the boundary should have the following behaviour

$$\phi \simeq \phi_- e^{-\Delta_- w} + \dots + \phi_+ e^{\Delta_+ w/\ell} + \dots \quad (4.21)$$

It is interesting to note that the BTZ black hole in the Poincaré like coordinates can be related with the AdS<sub>3</sub> spacetime. Thus, coming to the Poincaré coordinates in (4.10) and doing the change  $r_h^2 = -1$  we get an answer for the scalar field in the AdS<sub>3</sub> spacetime:

$$\Phi(r) = {}_2F_1\left(\frac{\Delta_-}{2}, \frac{\Delta_+}{2}, 1, 1 + r^2\right), \quad (4.22)$$

that is in agreement with an analysis from [38, 39] up to change of the radial variables (as  $\tan^{-1} r = \rho$ ,  $\tan \rho = \sinh \mu$ ).

## 5 Discussion

In this work, we have studied holographic renormalization group flows at finite temperature in the 3-dimensional truncated supergravity with a scalar potential. These RG flows are thermal generalizations of RG flows from [32] triggered by either relevant deformations or non-zero VEV of the operator.

For the potential with one extremum ( $a^2 \leq \frac{1}{2}$ ), the constructed thermal holographic RG flows correspond to the deformation of the dual theory by the relevant operator. The flows are described by asymptotically AdS black holes with the scalar field, which behaves monotonically and  $\phi_h$  at the horizon can take any value from the domain of definition of

the potential. For the case of the potential with several extrema ( $\frac{1}{2} \leq a^2 < 1$ ), we have constructed numerically thermal holographic RG flows, which are related with deformation of the dual conformal theory both by the relevant operator and by a nonzero VEV of the scalar operator. The former flows are characterized by a monotonic scalar field, as we have seen for the case of one extremum,  $a^2 \leq \frac{1}{2}$ . For them the value of the scalar field at the horizon  $\phi_h$  can take a value between the extrema of the potential. RG flows associated with a fixed point deformation by a non-zero expected mean of the operator are characterized by a non-monotonic behavior of the scalar field associated with a non-renormalizable contribution on the conformal boundary. It is shown that the scalar field on the horizon for such flows takes values near additional extrema.

For the thermal RG flows related with the relevant deformations we have found analytic solutions in the near-horizon regions. Using them we have studied the thermodynamics and have shown that at the extrema of the potential the thermodynamics is conformal.

For the monotonic slowly changing scalar field we have found a special class of the flows, which geometry is described by the non-rotating BTZ metric, and the solution for the scalar field is a solution of the hypergeometric equation. From the numerical observations we have shown that the solution for a scalar field can be extended from the horizon to the boundary. From the expansion of the scalar field solution on the boundary we have seen the correct behaviour.

It will further be interesting, to explore thermal two-point correlation functions [40, 41] in these geometries.

## Acknowledgments

AG and MP would like to thank Irina Ya. Aref'eva and Lev Astrakhantsev for useful discussions. The work of AG is supported by the Russian Science Foundation under Grant Number 20-12-00200.

## A Exact holographic RG flow

For the model (2.1) the exact domain wall solution, which preserve half of supersymmetries exists and was obtained in the work [27]. The scale factor of this solution reads

$$A_{\text{susy}} = \frac{1}{4a^2} \ln(e^{4a^2w} - 1), \quad (\text{A.1})$$

the scalar field is given by

$$\phi_{\text{susy}} = \frac{1}{2} \ln \left( \frac{1 + e^{-2a^2w}}{1 - e^{-2a^2w}} \right), \quad (\text{A.2})$$

where the radial coordinate  $w$  runs from 0 to  $\infty$ .

The metric of the domain wall solution with (A.1) can be represented as follows

$$ds_{\text{susy}}^2 = (e^{4a^2w} - 1)^{\frac{1}{2a^2}} (-dt^2 + dx^2) + dw^2. \quad (\text{A.3})$$

The domain wall solution (A.3) with (A.2) has an AdS asymptotics with  $w \rightarrow \infty$ , while if one send  $w$  to zero, the solution has a singular geometry. For  $a^2 \leq \frac{1}{2}$  this singular behaviour turns to be acceptable since the solution satisfies the Gubser's bound.

$$\phi \simeq \phi_{UV} + j\ell^{d-\Delta} e^{-(d-\Delta)w/\ell}, \quad w \rightarrow \infty, \quad (\text{A.4})$$

where in our case an UV fixed point is at  $\phi = 0$ ,  $\Delta = 1 \pm |1 - 2a^2|$ , so if  $a^2 < \frac{1}{2}$  the conformal dimension  $\Delta = 2(1 - a^2)$  and if  $\frac{1}{2} < a^2 < 1$  we have  $\Delta = 2a^2$ .

$$\Delta_- = d - \Delta = 2a^2, \quad \text{if } a^2 < \frac{1}{2}, \quad (\text{A.5})$$

$$\Delta_- = d - \Delta = 2 - 2a^2, \quad \text{if } \frac{1}{2} < a^2 < 1. \quad (\text{A.6})$$

The parameter  $\ell$  is the radius of the AdS spacetime  $\ell = \sqrt{-\frac{2}{V(\phi_{UV})}}$ . Then one can write

$$\phi \simeq \phi_{UV} + j\ell^{2a^2} e^{-2a^2w/\ell}, \quad w \rightarrow \infty, \quad (\text{A.7})$$

In our case  $V(\phi_{UV}) = V(0) = 2\Lambda$ . Setting  $\ell_{UV} = 1$ , we get  $\Lambda = -1$ . The Taylor series expansion of the Deger solution gives

$$\phi \simeq \phi_{UV} + e^{-2a^2w}, \quad w \rightarrow \infty. \quad (\text{A.8})$$

## B BTZ black hole in various coordinates

The metric of the non-rotating BTZ black hole in the domain-wall coordinates

$$ds^2 = e^{2\sqrt{-\frac{V(\phi_h)}{2}}w} \left( -(1 - e^{-\sqrt{-2V(\phi_h)}(w-w_h)})dt^2 + d\phi^2 \right) + \frac{dw^2}{1 - e^{-\sqrt{-2V(\phi_h)}(w-w_h)}}. \quad (\text{B.1})$$

where the blackening function given by

$$f(w) = 1 - e^{-\sqrt{-2V(\phi_h)}(w-w_h)}. \quad (\text{B.2})$$

with  $\ell = 1$ . Coming to the Poincaré coordinates with  $dw = \frac{dr}{r}$ , we get

$$ds^2 = e^{2\ln r} \left( -(1 - e^{-2(\ln r - \ln r_h)}) dt^2 + d\phi^2 \right) + \frac{dr^2}{r^2(1 - e^{-2(\ln r - \ln r_h)})}. \quad (\text{B.3})$$

that can be brought into the following form

$$ds^2 = -(r^2 - r_h^2) dt^2 + r^2 dx^2 + \frac{dr^2}{(r^2 - r_h^2)}. \quad (\text{B.4})$$

Remembering that the AdS<sub>3</sub> spacetime in terms of global coordinates with  $\ell = 1$  has the form

$$ds^2 = -(r^2 + 1) dt^2 + r^2 d\phi^2 + \frac{dr^2}{r^2 + 1}. \quad (\text{B.5})$$

## References

- [1] J. M. Maldacena, “The Large N limit of superconformal field theories and supergravity,” *Adv. Theor. Math. Phys.* **2** (1998) 231–252, [arXiv:hep-th/9711200](#).
- [2] E. Witten, “Anti-de Sitter space and holography,” *Adv. Theor. Math. Phys.* **2** (1998) 253–291, [arXiv:hep-th/9802150](#).
- [3] S. S. Gubser, I. R. Klebanov, and A. M. Polyakov, “Gauge theory correlators from noncritical string theory,” *Phys. Lett. B* **428** (1998) 105–114, [arXiv:hep-th/9802109](#).
- [4] E. T. Akhmedov, “A Remark on the AdS / CFT correspondence and the renormalization group flow,” *Phys. Lett. B* **442** (1998) 152–158, [arXiv:hep-th/9806217](#).
- [5] J. de Boer, E. P. Verlinde, and H. L. Verlinde, “On the holographic renormalization group,” *JHEP* **08** (2000) 003, [arXiv:hep-th/9912012](#).
- [6] D. Z. Freedman, S. S. Gubser, K. Pilch, and N. P. Warner, “Renormalization group flows from holography supersymmetry and a c theorem,” *Adv. Theor. Math. Phys.* **3** (1999) 363–417, [arXiv:hep-th/9904017](#).
- [7] S. de Haro, S. N. Solodukhin, and K. Skenderis, “Holographic reconstruction of space-time and renormalization in the AdS / CFT correspondence,” *Commun. Math. Phys.* **217** (2001) 595–622, [arXiv:hep-th/0002230](#).
- [8] M. Bianchi, D. Z. Freedman, and K. Skenderis, “Holographic renormalization,” *Nucl. Phys. B* **631** (2002) 159–194, [arXiv:hep-th/0112119](#).
- [9] M. Bianchi, D. Z. Freedman, and K. Skenderis, “How to go with an RG flow,” *JHEP* **08** (2001) 041, [arXiv:hep-th/0105276](#).
- [10] K. Skenderis, “Lecture notes on holographic renormalization,” *Class. Quant. Grav.* **19** (2002) 5849–5876, [arXiv:hep-th/0209067](#).
- [11] I. Papadimitriou and K. Skenderis, “AdS / CFT correspondence and geometry,” *IRMA Lect. Math. Theor. Phys.* **8** (2005) 73–101, [arXiv:hep-th/0404176](#).
- [12] I. Papadimitriou and K. Skenderis, “Correlation functions in holographic RG flows,” *JHEP* **10** (2004) 075, [arXiv:hep-th/0407071](#).

- [13] I. Papadimitriou, “Multi-Trace Deformations in AdS/CFT: Exploring the Vacuum Structure of the Deformed CFT,” *JHEP* **05** (2007) 075, [arXiv:hep-th/0703152](#).
- [14] U. Gürsoy, E. Kiritsis, L. Mazzanti, and F. Nitti, “Holography and Thermodynamics of 5D Dilaton-gravity,” *JHEP* **05** (2009) 033, [arXiv:0812.0792 \[hep-th\]](#).
- [15] A. Donos, J. P. Gauntlett, C. Rosen, and O. Sosa-Rodriguez, “Boomerang RG flows with intermediate conformal invariance,” *JHEP* **04** (2018) 017, [arXiv:1712.08017 \[hep-th\]](#).
- [16] I. Aref’eva and K. Rannu, “Holographic Anisotropic Background with Confinement-Deconfinement Phase Transition,” *JHEP* **05** (2018) 206, [arXiv:1802.05652 \[hep-th\]](#).
- [17] I. Y. Aref’eva, A. A. Golubtsova, and G. Policastro, “Exact holographic RG flows and the  $A_1 \times A_1$  Toda chain,” *JHEP* **05** (2019) 117, [arXiv:1803.06764 \[hep-th\]](#).
- [18] U. Gürsoy, E. Kiritsis, F. Nitti, and L. Silva Pimenta, “Exotic holographic RG flows at finite temperature,” *JHEP* **10** (2018) 173, [arXiv:1805.01769 \[hep-th\]](#).
- [19] Y. Bea and D. Mateos, “Heating up Exotic RG Flows with Holography,” *JHEP* **08** (2018) 034, [arXiv:1805.01806 \[hep-th\]](#).
- [20] I. Y. Aref’eva, “Holographic renormalization group flows,” *Theor. Math. Phys.* **200** no. 3, (2019) 1313–1323.
- [21] I. Y. Aref’eva, A. Hajilou, P. Slepov, and M. Usova, “Running coupling for holographic QCD with heavy and light quarks: Isotropic case,” *Phys. Rev. D* **110** no. 12, (2024) 126009, [arXiv:2402.14512 \[hep-th\]](#).
- [22] A. F. Faedo, C. Hoyos, M. Piai, R. Rodgers, and J. G. Subils, “Light holographic dilatons near critical points,” [arXiv:2406.04974 \[hep-th\]](#).
- [23] A. Frenkel, S. A. Hartnoll, J. Kruthoff, and Z. D. Shi, “Holographic flows from CFT to the Kasner universe,” *JHEP* **08** (2020) 003, [arXiv:2004.01192 \[hep-th\]](#).
- [24] E. Cáceres, A. Kundu, A. K. Patra, and S. Shashi, “Trans-IR flows to black hole singularities,” *Phys. Rev. D* **106** no. 4, (2022) 046005, [arXiv:2201.06579 \[hep-th\]](#).
- [25] E. Cáceres, A. K. Patra, and J. F. Pedraza, “Shock waves, black hole interiors and holographic RG flows,” *JHEP* **07** (2024) 052, [arXiv:2311.12940 \[hep-th\]](#).
- [26] N. S. Deger, A. Kaya, E. Sezgin, and P. Sundell, “Matter coupled AdS(3) supergravities and their black strings,” *Nucl. Phys. B* **573** (2000) 275–290, [arXiv:hep-th/9908089](#).



- [27] N. S. Deger, “Renormalization group flows from  $D = 3$ ,  $N=2$  matter coupled gauged supergravities,” *JHEP* **11** (2002) 025, [arXiv:hep-th/0209188](#).
- [28] A. Golubtsova, A. Nikolaev, and M. Podoinitsyn, “Holographic RG flows in a 3D gauged supergravity at finite temperature,” *Phys. Rev. D* **110** no. 6, (2024) 066011, [arXiv:2405.06515 \[hep-th\]](#).
- [29] N. S. Deger and O. Sarioglu, “Supersymmetric strings and waves in  $D = 3$ ,  $N=2$  matter coupled gauged supergravities,” *JHEP* **12** (2004) 039, [arXiv:hep-th/0409169](#).
- [30] N. S. Deger and O. Sarioglu, “New Supersymmetric Solutions in  $N=2$  Matter Coupled AdS(3) Supergravities,” *JHEP* **08** (2006) 078, [arXiv:hep-th/0605098](#).
- [31] A. A. Golubtsova and M. K. Usova, “Stability analysis of holographic RG flows in 3d supergravity,” *Eur. Phys. J. Plus* **138** no. 3, (2023) 260, [arXiv:2208.01179 \[hep-th\]](#).
- [32] K. Arkhipova, L. Astrakhantsev, N. S. Deger, A. A. Golubtsova, K. Gubarev, and E. T. Musaev, “Holographic RG flows and boundary conditions in a 3D gauged supergravity,” *Eur. Phys. J. C* **84** no. 6, (2024) 560, [arXiv:2402.11586 \[hep-th\]](#).
- [33] J. Sonner and P. K. Townsend, “Dilaton domain walls and dynamical systems,” *Class. Quant. Grav.* **23** (2006) 441–464, [arXiv:hep-th/0510115](#).
- [34] A. Golubtsova, “Holographic RG flow at zero and finite temperatures,” *EPJ Web Conf.* **191** (2018) 05012.
- [35] The Sage Developers, *SageMath, the Sage Mathematics Software System (Version 10.5)*, 2024. <https://www.sagemath.org>.
- [36] L. Perko, *Differential equations and dynamical systems*. Springer-Verlag, Berlin, Heidelberg, 1991.
- [37] P. Kraus, “Lectures on black holes and the AdS(3) / CFT(2) correspondence,” *Lect. Notes Phys.* **755** (2008) 193–247, [arXiv:hep-th/0609074](#).
- [38] V. Balasubramanian, P. Kraus, and A. E. Lawrence, “Bulk versus boundary dynamics in anti-de Sitter space-time,” *Phys. Rev. D* **59** (1999) 046003, [arXiv:hep-th/9805171](#).
- [39] D. Z. Freedman, S. D. Mathur, A. Matusis, and L. Rastelli, “Correlation functions in the CFT(d) / AdS(d+1) correspondence,” *Nucl. Phys. B* **546** (1999) 96–118, [arXiv:hep-th/9804058](#).
- [40] D. Rodriguez-Gomez and J. G. Russo, “Correlation functions in finite temperature CFT and black hole singularities,” *JHEP* **06** (2021) 048, [arXiv:2102.11891 \[hep-th\]](#).

- [41] D. Rodriguez-Gomez and J. G. Russo, “Thermal correlation functions in CFT and factorization,” *JHEP* **11** (2021) 049, [arXiv:2105.13909 \[hep-th\]](#).